Obtaining of Zinc Oxide Nanoparticles Modified With Galactose and Assessment of Their Cytotoxic Properties

Jolanta Pulit-Prociak (jolanta.pulit-prociak@pk.edu.pl)
Cracow University of Technology https://orcid.org/0000-0001-5005-7134
Anita Staroń
Cracow University of Technology
Olga Długosz
Cracow University of Technology
Dominik Domagała
University of Agriculture in Krakow
Katarzyna Janczyk
Cracow University of Technology
Marcin Banach
Cracow University of Technology

Research

Keywords: nanomaterials, zinc oxide, galactose, toxicity

Posted Date: October 12th, 2021

DOI: https://doi.org/10.21203/rs.3.rs-958898/v1

Abstract

The work presents the method for preparation of zinc oxide nanoparticles with galactose coating. Bare zinc oxide nanoparticles are well-known and popular drug delivers. However, the fact that zinc ions may be released from their structure easily, they may pose a threat to the living organism. Thus the modification of such a product has been performed. The physicochemical properties of the products have been analysed. XRD technique revealed crystallographic structure of the products. Based on ATR-FTIR analysis it was confirmed that galactose has been successfully attached to the zinc oxide nanoparticles. TEM-EDS microscopy was applied in order to assess the shape of nanoparticles and also for the confirmation of galactose on the particles surface. The releasing of zinc ions from the modified products was compared to their releasing from basic, non-modified sample. Also, cytotoxicity and proliferation of obtained products have been analysed with using Chinese hamster ovary cells. It was found out that the proposed technology may lead to obtain stable forms of modified zinc oxide nanoparticles with limited toxicity.

1. Introduction

Nanaotechnology has been attracting interest for several decades. Nanoparticles and nanopores are structures in which at least one of the three dimensions is less than 100 nanometers [1]. They may have an ordered crystal structure, be monocrystals or their particles may be arranged as in the case of a glassy metal, i.e. randomly [2]. The size of materials at the nanoscale also offers the possibility of altering their structures in such a way as to obtain beneficial, previously unseen chemical or biological properties [3][4]. The size of materials at the nanoscale also offers the possibility of altering their structures in such a way as to obtain beneficial, previously unseen chemical or biological properties [5] [6]. Medicine is a field of science where nanoscale materials are of particular importance, both natural and synthetic. In this case, however, the greatest attention is paid to their structure, due to the fact that they are used in medical diagnostics and active substance transport systems [7] [8].

Nanoparticles to be introduced into the body as carriers should be characterized by several properties. First of all, during transport, the activity of the transferred active substance should not be significantly reduced. The drug should be released in a controlled manner, at a more precise time, only In the course of targeted therapy, the drug should be released in a controlled manner, at a more precise time, only in the designated, infected cells, bypassing healthy tissues. The drug concentration administered is much lower compared to conventional chemotherapy [9][10]. The most commonly used system is passive transport. It consists in the spontaneous passage of conjugates through cell membranes. Infected tissues are usually larger than healthy ones, leaky and have a defective lymphatic drainage system. Thanks to this, nanoscale structures can enter and destroy cancer cells. Active transport is a constantly improving drug delivery system. A modifier (protein, polymer, carbohydrate, etc.) is attached to the surface structure of the carrier, which constitutes a kind of tumor receptor and leads the active substance directly to its cells. Compared with traditional treatment, the concentration of the antibiotic in infected structures is up to 50 times higher [11], [12], [13]. Structural modifications and the use of different oxide preparation methods

affect its biological properties. The literature reports several routes for the chemical formation of zinc nanoparticles. One way is precipitation in microemulsions. It is a simple, harmless method in which structures of uniform particle size can be obtained of uniform particle size [14]. Sol-gel technology is a widespread method for obtaining metal oxides. The process involves the conversion of a precursor solution into a sol, then a gel, and thermal treatment of the product. The sol-gel method is simple and relatively inexpensive, leads to high purity products with hexagonal structure [15][16].

The most common method of obtaining crystalline ZnO is its precipitation from salt solutions. By changing the concentration, temperature or pH, a myriad of modifications and properties of such nanoparticles can be obtained. The hydrothermal method consists in the synthesis of ZnO at elevated pressure and temperature. Apart from chemical methods, zinc oxide may be obtained physically, e.g. during spray pyrolysis or biologically from plant extracts [14], [17]. Zinc oxide in small amounts is safe for humans. It is used as an antimicrobial agent in food, water disinfection, medicinal and cosmetic industry. Its action is to damage the cell membranes of microorganisms, which increases their permeability [18], [19]. According to another mechanism, absorption of sufficient energy by zinc oxide nanoparticles results in the formation of a free electron. This can absorb water and form so-called hydroxyl radicals. When interacting with oxygen, a superoxide ion is formed, which can then transform into an identical radical. This structure has been shown to damage the cell wall and cause oxidative stress [20], [21].

Functionalization of particles by various substances significantly affects the properties of the carriers as well as the drugs themselves. The uptake of particles modified with sugars, by cancer cells, is much higher compared to unaltered surfaces. Appropriate modification of the carrier surface can also reduce its toxicity [22], [23]. An increase in carbonyls resulted in an increase in oxidative stress in cells. The level of infection was strongly dependent on the amount of reactive oxygen species measured as protein carbonyls, but not on the rate of nanoparticle uptake by cells [24]. Cancer cells have a higher affinity for positively charged nanoparticles. The surface charge therefore significantly affects their cellular uptake [25] [26]. The attachment of amino acids, on the other hand, can therefore increase the uptake of nanocarriers, lengthen their sequences and add stability. The presence of different ligands thus affects the toxicity of the structures, as does the synthesis process and the amount of impurities present. The high bioavailability of the formed nanoparticles was also confirmed during the study [27].

The aim of the study was to obtain zinc oxide nanoparticles modified by attaching galactose to their surface. Thanks to that it would be possible to inhibit releasing of zinc that may lead to formation of ROS and thus such a construct may be found as safer for a living organism.

2. Materials And Methods

2.1. Materials

The following compounds were used in this study: zinc chloride (99.0%), sodium hydroxide (≥98.-%), D-(+)-galaktoza (≥99.0%), tannic acid (p.p.a.). All compounds were obtained from Sigma-Aldrich. All

aqueous solutions were prepared using deionized water (Polwater, 0.18 µS). CHO cell line, culture media (F-12K Medium) and supplements (FBS, antibiotics) were obtained from Sigma-Aldrich, LDH cytotoxicity assay Kit was obtained from Thermo Fisher Scientific and BrdU cell proliferation kit was obtained from Roche.

2.2. Methods

The method of producing a series of modified zinc oxide nanoparticles was based on the performance of precipitation and dehydration processes. Zinc chloride served as the source of zinc ions. The precipitating agent was sodium hydroxide. In order to modify the surface of zinc oxide nanoparticles, D-(+)-galactose was used. Nine different products which differed in the process parameters for their preparation have been obtained. Initially, the aqueous sodium hydroxide solution was added dropwise to the aqueous solution of zinc chloride which was in a 100 ml Teflon vessel. In addition, some processes used tannic acid to further stabilize nanoparticles. The obtained mixture was homogenized for 60 seconds (Hielscher UP400St, 40W). Then, the aqueous solution of galactose was introduced into the reaction mixture and the whole was homogenized again for additional 60 seconds. The concentrations and volumes of the individual solutions were so calculated as the theoretical weight of zinc oxide was equal to 1.01725 g (0.0125 mole). Later, the Teflon vessel has been placed into the Magnum II microwave reactor (Ertec Poland) which was in order to carry out the zinc hydroxide dehydration process. The process temperature was equal to 150˚C and the process time (after reaching this temperature) was equal to 5 minutes. After completion of the process, the product was filtered off and washed with deionized water twice. The filtrate was discarded and the solid product was dried in a laboratory drier at 80˚C. The dried products have been triturated in an agate mortar to make them homogeneous. The laboratory work has been planned with applying Design of Experiments (DoE) technique. The input parameters were: the molar ratio of galactose to zinc oxide (n Gal : n ZnO) which was 0.02, 0.11 or 0.2, the fold ratio of the stoichiometric sodium hydroxide to zinc nitrate which was 1, 2 or 3 and the molar ratio of tannic acid to zinc oxide (if any) (n tan. acid : n ZnO) which was 0, 0.01 or 0.02. Table 1 shows the process parameters. A reference product without modifier (galactose) was also prepared.

Table 1
Process parameters (according to DoE)

Sample	n GAL : n ZnO	fold of NaOH vs. stoichiometric amount	n tan. acid : n ZnO
G1	0.02	1	0.00
G2	0.02	2	0.02
G3	0.02	3	0.01
G4	0.11	1	0.02
G5	0.11	2	0.01
G6	0.11	3	0.00
G7	0.20	1	0.01
G8	0.20	2	0.00
G9	0.20	3	0.02
G/Base	0.00	1	0

The physicochemical properties of the obtained products were analysed. In order to confirm the crystallographic structure of zinc oxide, XRD technique has been applied (X'Pert PW 1752/00, Philips). X-ray diffraction (XRD) data analysis was performed with Match! software using the Rietveld refinement technique. Rietveld refinement of XRD patterns was carried out by considering the Pseudo-Voigt function. In order to prove the presence of carbon on the nanoparticles surface, ATR-FTIR analysis has been used (Nicolet 380 spectrophotometer, Thermo Fisher). It was the indirect evidence of the incorporation of galactose. The size and shape of nanoparticles were assessed by TEM-EDS microscopy (Tecnai TEM G2 F20X-Twin 200 kV, FEI). Size and electrokinetic potential of zinc oxide nanoparticles suspended in aqueous medium (10 ppm) was assessed by applying DLS technique (Zetasizer Nano ZS, Malvern Instruments Ltd). The suspensions have been homogenized for 1 minute prior to analysis.

2.2.1. Analysis of zinc ions releasing from the obtained products

The releasing of zinc ions from both the modified and basic products was performed. For this purpose, about 0.02 g of the sample was weighed into a polystyrene container with an accuracy of 0.0001 g. The proper amount of distilled water was added to that in order to obtain a 0.5% (w/v) suspension. The whole was mixed at 37°C on a multi-station magnetic stirrer for a specified time (1, 3, 5, 10, 20, 40, 80 min). Upon this time intervals, the suspensions were withdrawn with syringes and filtered through nitrocellulose syringe filters (0.45 μm). The filtrates were analysed by Atomic Absorption Spectrometry (ASA 370, Perkin Elmer). Based on the concentration of released zinc it was possible to determine the releasing rate form the obtained materials.

2.2.2. In Vitro Cell viability assay

Also, cytotoxicity and proliferation of obtained products have been analysed with using Chinese hamster ovary cells. It was found out that the proposed technology may lead to obtain stable forms of modified zinc oxide nanoaprticles with limited toxicity.

Chinese hamster ovary (CHO) cells (Sigma-Aldrich, cat no. 85051005) were cultured in F-12K Medium (Sigma-Aldrich, cat no. N4888), with 10% Fetal Bovine Serum (FBS) and antibiotics: penicillin and streptomycin (Sigma-Aldrich, cat no. P4333) and stored in an incubator (NuAire, Plymouth, MN, USA) at 37°C and 5% CO_2. The culture medium was replaced with fresh every 2-3 days, passage was made when 80% confluence was reached.

Cytotoxicity analysis using lactate dehydrogenase (LDH) consisted in measuring the activity of the enzyme released into the culture medium during cell death. The measure of the extracellular activity of LDH in the medium is an enzymatic reaction in which LDH catalyzes the conversion of lactate to pyruvate by reducing NAD^+ to NADH (nicotinamide adenine dinucleotide). NADH, then reduces the tetrysoline to a colored formazan, the amount of which has been measured spectrophotometrically at 490 nm. The concentration of formazan in the culture medium is directly proportional to the amount of LDH released. In the experiment, the absorbance of the samples was measured on a Multiskan GO (Thermo Fisher Scientific) microplate reader.

In the cytotoxicity assay, CHO cells were seeded at 9×10^3 cell per well in 150 µl on 96-well plates and grown in culture medium for 24 hours. Then the medium was replaced with fresh, containing nanomaterials in concentration 80, 70, 50, 30 and 10 µg/ml and cultured for next 24, 48 and 72 hours. Cells grown in standard medium were used as a negative control of cytotoxicity. The cytotoxicity assessment of nanomaterials was performed using the Pierce LDH Cytotoxicity Assay Kit (Thermo Fisher Scientific, cat no 88954), according to the protocol provided by the manufacturer. The absorbance was measured at two wavelengths - 490 nm (formazan absorbance) and 680 nm (background absorbance). The cytotoxicity was calculated from the formula:

$$\%\ \text{Cytotoxicity} = \frac{\text{Compound-treated LDH activity} - \text{Spontaneous LDH activity}}{\text{Maximum LDH activity} - \text{Spontaneous LDH activity}} \cdot 100$$

Cell proliferation was determined using a Cell Proliferation ELISA kit, BrdU (Roche, cat no. 11647229001). The test consists of quantifying DNA synthesis. Bromodeoxyuridine (BrdU) is a synthetic analogue of the thymidine nucleoside that is incorporated into the DNA of a dividing cell during the S phase of its division. The detection of BrdU with the use of a specific antibody conjugated with an enzyme and the enzymatic reaction of the above enzyme with a chromogenic substrate allows for a colorimetric analysis of the proliferative capacity of cells. The amount of the product formed was measured spectrophotometrically. The absorbance was measured at two wavelengths - 450 nm (product absorbance) and 690 nm (background absorbance). A positive BrdU result (high signal) proves the viability and functionality of a given cell line. The absorbance of the samples was measured on a Multiscan GO (Thermo Fisher Scientific) microplate reader.

In the proliferation assay, CHO cells were seeded at 9×10^3 cell per well in 150 µl on 96-well plates and grown in culture medium for 24 hours. Then the medium was replaced with fresh, containing nanomaterials and cultured for next 24, 48 and 72 hours. Cells grown in standard medium were used as a control. Cell proliferation was determined using a commercially available Cell Proliferation ELISA kit, BrdU (Roche, Cat # 11647229001) according to the protocol provided by the manufacturer.

3. Results

Figure 1 shows the XRD spectra of all prepared products. The diffractograms of pure zinc oxide and modified products do not differ from each other. There are visible peaks characteristic for zinc oxide at 31.7, 34.4, 36.3, 47.4 and 56.5°, which confirm the obtaining of zinc oxide in all materials. Modification of the products with galactose and tannic acid did not affect the purity of the obtained materials.

The Rietveld method is a well-established technique for extracting structural details from powder diffraction data. The method uses a least squares procedure to compare Bragg intensities and those calculated from a possible structural model. The quality of fit of the experimental data is assessed by calculating parameters such as χ^2 and R_B (Bragg coefficient).

The phase composition of the materials was assessed by applying the Rietveld method. All products are in a hexagonal structure, i.e. hexagonal/P 63 m c (186). In all materials the crystalline phase was made in 100% of ZnO.

The obtained fractional atomic positions are given in Table 2. All materials had positions the same positions of specific coordinates.

The resulting fit coefficients are shown in Table 3.

Table 2
Fractional atomic positions

Material	Atoms	x	y	z
G1 – G9, G/Base	Zn	0,333	0,667	0,000
	O	0,333	0,667	0,382

Tab. 3. Fitting coefficients

Material	R_B [%]	χ^2	a [Å]	c [Å]
G1	4,9	4,2	3,2520	5,2097
G2	4,8	2,9	3,2483	5,2039
G3	6,0	5,9	3,2413	5,1905
G4	14,3	4,2	3,2427	5,1871
G5	5,3	6,9	3,2602	5,2229
G6	3,5	4,0	3,2511	5,2081
G7	4,6	3,6	3,2494	5,2054
G8	4,1	3,8	3,2513	5,2080
G9	5,1	4,7	3,2523	5,2097
G/Base	2,5	5,1	3,2515	5,2092

R_B – Bragg factor, χ^2 – goodness of fit factor, a, c – lattice constants

Bond lengths and angles were calculated using refined lattice parameters and fractional coordinates using Diamond software. A typical elemental cell showing bond lengths for the G3 sample is shown in Figure 2. All obtained materials were characterised by the same elemental cells.

The diffractograms of the obtained materials together with the fitted graphs based on the Rietveld method are shown in Figure 3A-J. The experimental data are shown as blue dots and the calculated intensities are shown as a black continuous line. The lower line represents the difference between the measured and calculated intensities. It was found out that the difference is not significant and the refinement may be assessed as good one.

Analysis of crystallite size was performed using XRD peak width. The crystallite size was calculated using Scherrer's formulae. The Scherrer formula is defined as:

$d_{Sch}=k\lambda/\beta\cos\theta$

where the constant k depends on the shape of the crystallite size, β is the width at half maximum peak describing the material, λ is the wavelength of CuKa radiation, θ is the Bragg diffraction angle and d_{Sch} is the crystallite size. The results are presented in Figure 3K.

Based on statistical analysis of an experiment with three-lever input factors, it was found that crystallite size was dependent on all process parameters. When the molar ratio of galactose to zinc oxide was enhancing, the size of crystallites was reducing. The same dependence was characterised for the molar ratio of tannic acid to zinc oxide. However the greatest fold of NaOH vs. stoichiometric amount was, the size of crystallites was also greater. The highest value of desirability (1.0) was corresponding to the lowest crystallites size. In order to obtain the smallest crystallites the process should be conducted with the following parameters: n Gal : n ZnO = 0.2, fold of NaOH vs. stoichiometric amount = 1 and n tan. acid : n ZnO = 0.02 (Fig. 4). These results are in line with predictions that the presence of organic matter inhibits the growth of crystallites.

For a more precise analysis of the obtained structures, the ATR-FTIR spectroscopy of selected products was measured. Figure 5 presents the ATR-FTIR spectra for the reference material and the G7 sample, which contained both galactose and tannic acid. The peaks corresponding to the hydroxyl group are at approx. 3370 cm^{-1}. They come from adsorbed water (pure zinc oxide) and from the hydroxyl groups present in tannic acid - in the spectra for G7 sample this peak is significantly more intense. There are many significant peaks between the wavelengths of 1650-500 cm^{-1}, the source of which is tannic acid. Above 1260 cm^{-1} there are peaks of carboxyl groups corresponding to gallic acid molecules which are contained in the structure of tannic acid. The presence of C-C, C-O and C = O bonds is confirmed by the peaks at 826, 1347 and 1684 cm^{-1}. The groups characteristic of galactose can be identified on the basis of the following peaks: 1015 cm^{-1} (OH), 1205 cm^{-1} (C-O-C) and 1345 cm^{-1} (CH_2).

The work also includes TEM-EDS analysis. Its results are shown in Figure 3. This was performed for the pure zinc oxide and the G6 sample. Nanometric ZnO has elongated and irregular shapes, resembling snowflakes. The average particle size in the smallest dimension does not exceed 200 nm. Its surface is irregular. Elemental analysis showed that the material contains zinc and oxygen in amounts close to the theoretical composition of pure ZnO (Figure 6A). Figure 6B shows the results of TEM-EDS analysis for product G6. The shape of the particles is also irregular, but rod-shaped inclusions are visible, whose size in one dimension is about 50 nm. EDS analysis confirmed the presence of organic matter in the material which is the confirmation for obtaining galactose coating on the surface.

DLS technique provided size of nanoparticles and their stability in aqueous medium by measuring electrokinetic potential, ζ. The size of obtained zinc oxide particles was different and it was in the range of 241 – 1866 nm (Fig. 7A). Passive cancer therapy takes advantage of the anatomical and physiological properties of a tumour. It is characterised by increased vascular permeability (leaky network of blood vessels). Scientists have determined that the diameter of the gaps ranges from 100 to 800 nm, while in healthy tissues only 2 - 6 nm. The average size of most anticancer drugs is small and does not exceed 10 nm. Using them in a stand-alone would cause them to diffuse equally into healthy and diseased tissues. Combining them with nanocarriers (50-800 nm) would significantly reduce or even eliminate the penetration of therapeutic substances into the structure of healthy tissues. Obtained results are satisfactory, since in some cases the size of nanoparticles was less than 800 nm (G1, G4, G6, G8 and

G9). What is more, the values of electrokinetic potential in almost all cases were greater than 20 mV, which means that aqueous suspensions of prepared nanometric powder are stable (Fig. 7B).

3.1. Results of analysis of zinc ions releasing from the obtained products

The results of zinc releasing from obtained modified nanoparticles are presented in Figure 8. It may be observed that in general, the modification of zinc oxide surface leads to limited elution of zinc ions. That means that galactose coating inhibits the solubility of the obtained products. Thus they are more stable in time. One should note that the releasing rate falls off exponentially with time. The greatest concentration of released zinc is determined immediately after starting elution process. This may be due to the fact that in the further time, the released zinc is being readsorbed on the zinc oxide surface.

3.2. Results of In Vitro Cell viability assay

The results of in vitro cell viability analysis are presented in Figures 9 and 10. The concentration dependent cytotoxicity of obtained nanoparticles in CHO cells (Fig. 6) shows that the greater concentration of nanoparticles in the tested suspension leads to the enhanced cytotoxic effect. What is more, one may observe that particles which are not modified (basic ones) exhibit more harmful effect on the cells. That is in line with the initial assumption. This is the confirmation for the fact that the galactose coating may inhibit the releasing of zinc which is the direct factor causing the toxic effect.

Figure 10 presents the results of both cytotoxicity and proliferation analysis for all products. The concentration of all analysed suspensions was equal to 50 mg/mL. In all cases the cytotoxicity for modified products was lower than in basic sample (G/Base). That means that ROS generation in those innovative products contribute to cell killing mechanism to a lesser extent. Concerning both factors assessing the cells viability, the best results have been obtained for G4 sample. In this case the cytotoxicity was equal to 1.94%, which was in 81% lower value than for basic material. The proliferation for this material was equal to 69.36% which is in over 76% better than for reference material. In general, all modified products led to achieve higher values of proliferation of Chinese hamster ovarian cells.

Concerning all results presented above one may conclude that the values of parameters that lead to obtain product with most desired physicochemical and utility properties are as follows: n GAL : n ZnO should be equal to 0.11:1.00 (medium value), fold of NaOH vs. stoichiometric amount should be equal to 1 and n tan. acid : n ZnO should be equal to 0.02:1.00 (the highest value). These processes parameters ensure production of zinc oxide nanoaprticles modified with galactose whose particle size does not exceed 800 nm (is equal to 445 nm) and the value electrokinetic potential of their aqueous suspension is satisfactory (ζ = 28.2 mV) it is the highest among measured.

4. Conclusion

The performed studies are the proof that it was possible to obtain stable zinc oxide nanoparticles modified with galactose which are characterized by limited releasing of zinc ions. The physicochemical properties of the modified products allow them to be used as possible drug delivery vehicles. The results of *in vitro* Cell viability assay showed that the cytotoxicity of modified products in relation to Chinese hamster ovarian cells is limited and the proliferation of those cells is enhanced while using the modified materials.

Declarations

Ethics approval and consent to participate

Not applicable.

Consent for publication

All authors consent for the manuscript to be published.

Availability of data and materials

All data generated or analysed during this study is available from corresponding author on reasonable request.

Competing interests

The authors declare that they have no competing interests.

Funding

This work is a part of the project “A method of producing non-toxic carriers of active substances based on nanomaterials,” supported by the National Centre for Research and Development, Poland under the agreement LIDER/20/0080/L-9/17/NCBR/2018.

Authors' contributions

JPP: concept, design and writing of the manuscript, AS: analysis of physicochemical properties of obtained products, writing of the manuscript, OD: analysis of crystallographic data, DD: performing of the cytotoxic studies, writing of the manuscript, KJ: preparation of materials, MB: interpretation of the obtained results. All authors read and approved the final manuscript.

Acknowledgements

We thank National Centre for Research and Development, Poland for the grants and financial support to this research.

References

[1] J. Jeevanandam, A. Barhoum, Y. S. Chan, A. Dufresne, and M. K. Danquah, “Review on nanoparticles and nanostructured materials: History, sources, toxicity and regulations,” *Beilstein Journal of Nanotechnology*, vol. 9, no. 1. Beilstein-Institut Zur Forderung der Chemischen Wissenschaften, pp. 1050–1074, 03-Apr-2018.

[2] R. Dobrucka, “Selected applications of metal nanoparticles in medicine and pharmacology,” *LogForum*, vol. 15, no. 4, pp. 449–457, 2019.

[3] K. Khalid *et al.*, “Advanced in developmental organic and inorganic nanomaterial: a review,” *Bioengineered*, vol. 11, no. 1, pp. 328–355, Jan. 2020.

[4] A. Ali *et al.*, “Review on Recent Progress in Magnetic Nanoparticles: Synthesis, Characterization, and Diverse Applications,” *Frontiers in Chemistry*, vol. 9. Frontiers Media S.A., p. 548, 13-Jul-2021.

[5] I. Khan, K. Saeed, and I. Khan, “Nanoparticles: Properties, applications and toxicities,” *Arabian Journal of Chemistry*, vol. 12, no. 7. Elsevier B.V., pp. 908–931, 01-Nov-2019.

[6] S. Sharma, S. Jaiswal, B. Duffy, and A. K. Jaiswal, “Nanostructured Materials for Food Applications: Spectroscopy, Microscopy and Physical Properties,” *Bioengineering*, vol. 6, no. 1. MDPI AG, 01-Mar-2019.

[7] A. Staroń, O. Długosz, J. Pulit-Prociak, and M. Banach, “Analysis of the Exposure of Organisms to the Action of Nanomaterials,” *Materials (Basel).*, vol. 13, no. 2, p. 349, Jan. 2020.

[8] J. K. Patra *et al.*, “Nano based drug delivery systems: Recent developments and future prospects ,” *Journal of Nanobiotechnology*, vol. 16, no. 1. BioMed Central Ltd., p. 71, 19-Sep-2018.

[9] A. Chowdhury, S. Kunjiappan, T. Panneerselvam, B. Somasundaram, and C. Bhattacharjee, “Nanotechnology and nanocarrier-based approaches on treatment of degenerative diseases,” *Int. Nano Lett.*, vol. 7, no. 2, pp. 91–122, Jun. 2017.

[10] Y. Peng *et al.*, “Research and development of drug delivery systems based on drug transporter and nano-formulation,” *Asian Journal of Pharmaceutical Sciences*, vol. 15, no. 2. Shenyang Pharmaceutical University, pp. 220–236, 01-Mar-2020.

[11] P. Boisseau and B. Loubaton, “Nanomedicine, Nanotechnology in medicine,” Jun. 2011.

[12] A. Ulldemolins *et al.*, “Perspectives of nano-carrier drug delivery systems to overcome cancer drug resistance in the clinics,” *Cancer Drug Resistance*, vol. 4, no. 1. OAE Publishing Inc., pp. 44–68, 19-Mar-2021.

[13] G. Tiwari *et al.*, “Drug delivery systems: An updated review,” *Int. J. Pharm. Investig.*, vol. 2, no. 1, p. 2, 2012.

[14] G. T. Mazitova, K. I. Kienskaya, D. A. Ivanova, I. A. Belova, I. A. Butorova, and M. V. Sardushkin, “Synthesis and Properties of Zinc Oxide Nanoparticles: Advances and Prospects,” *Rev. J. Chem.*, vol. 9, no. 2, pp. 127–152, Apr. 2019.

[15] S. Thiagarajan, A. Sanmugam, and D. Vikraman, “Facile Methodology of Sol-Gel Synthesis for Metal Oxide Nanostructures,” in *Recent Applications in Sol-Gel Synthesis*, InTech, 2017.

[16] I. Litzov and C. Brabec, “Development of Efficient and Stable Inverted Bulk Heterojunction (BHJ) Solar Cells Using Different Metal Oxide Interfaces,” *Materials (Basel).*, vol. 6, no. 12, pp. 5796–5820, Dec. 2013.

[17] M. A. Moghri Moazzen, S. M. Borghei, and F. Taleshi, “Change in the morphology of ZnO nanoparticles upon changing the reactant concentration,” *Appl. Nanosci.*, vol. 3, no. 4, pp. 295–302, Aug. 2013.

[18] A. Yoo, M. Lin, and A. Mustapha, “Zinc oxide and silver nanoparticle effects on intestinal bacteria,” *Materials (Basel).*, vol. 14, no. 10, p. 2489, May 2021.

[19] R. Brayner, R. Ferrari-Iliou, N. Brivois, S. Djediat, M. F. Benedetti, and F. Fiévet, “Toxicological impact studies based on Escherichia coli bacteria in ultrafine ZnO nanoparticles colloidal medium,” *Nano Lett.*, vol. 6, no. 4, pp. 866–870, Apr. 2006.

[20] B. Lallo da Silva *et al.*, “Relationship Between Structure And Antimicrobial Activity Of Zinc Oxide Nanoparticles: An Overview</p>,” *Int. J. Nanomedicine*, vol. Volume 14, pp. 9395–9410, Dec. 2019.

[21] E. Friehs *et al.*, “Toxicity, phototoxicity and biocidal activity of nanoparticles employed in photocatalysis,” *Journal of Photochemistry and Photobiology C: Photochemistry Reviews*, vol. 29. Elsevier B.V., pp. 1–28, 01-Dec-2016.

[22] I. Sur, D. Cam, M. Kahraman, A. Baysal, and M. Culha, “Interaction of multi-functional silver nanoparticles with living cells,” *Nanotechnology*, vol. 21, no. 17, Apr. 2010.

[23] N. Ivanova, V. Gugleva, M. Dobreva, I. Pehlivanov, S. Stefanov, and V. Andonova, “Silver Nanoparticles as Multi-Functional Drug Delivery Systems,” in *Nanomedicines*, IntechOpen, 2019.

[24] D. C. Kennedy *et al.*, “Carbohydrate functionalization of silver nanoparticles modulates cytotoxicity and cellular uptake,” *J. Nanobiotechnology*, vol. 12, no. 1, p. 59, Dec. 2014.

[25] C. G. Liu, Y. H. Han, R. K. Kankala, S. Bin Wang, and A. Z. Chen, “Subcellular performance of nanoparticles in cancer therapy,” *Int. J. Nanomedicine*, vol. 15, pp. 675–704, Feb. 2020.

[26] M. Sousa De Almeida, E. Susnik, B. Drasler, P. Taladriz-Blanco, A. Petri-Fink, and B. Rothen-Rutishauser, “Understanding nanoparticle endocytosis to improve targeting strategies in nanomedicine,” *Chemical Society Reviews*, vol. 50, no. 9. Royal Society of Chemistry, pp. 5397–5434, 07-May-2021.

[27] B. Harper *et al.*, “The Impact of Surface Ligands and Synthesis Method on the Toxicity of Glutathione-Coated Gold Nanoparticles,” *Nanomaterials*, vol. 4, no. 2, pp. 355–371, May 2014.

Figures

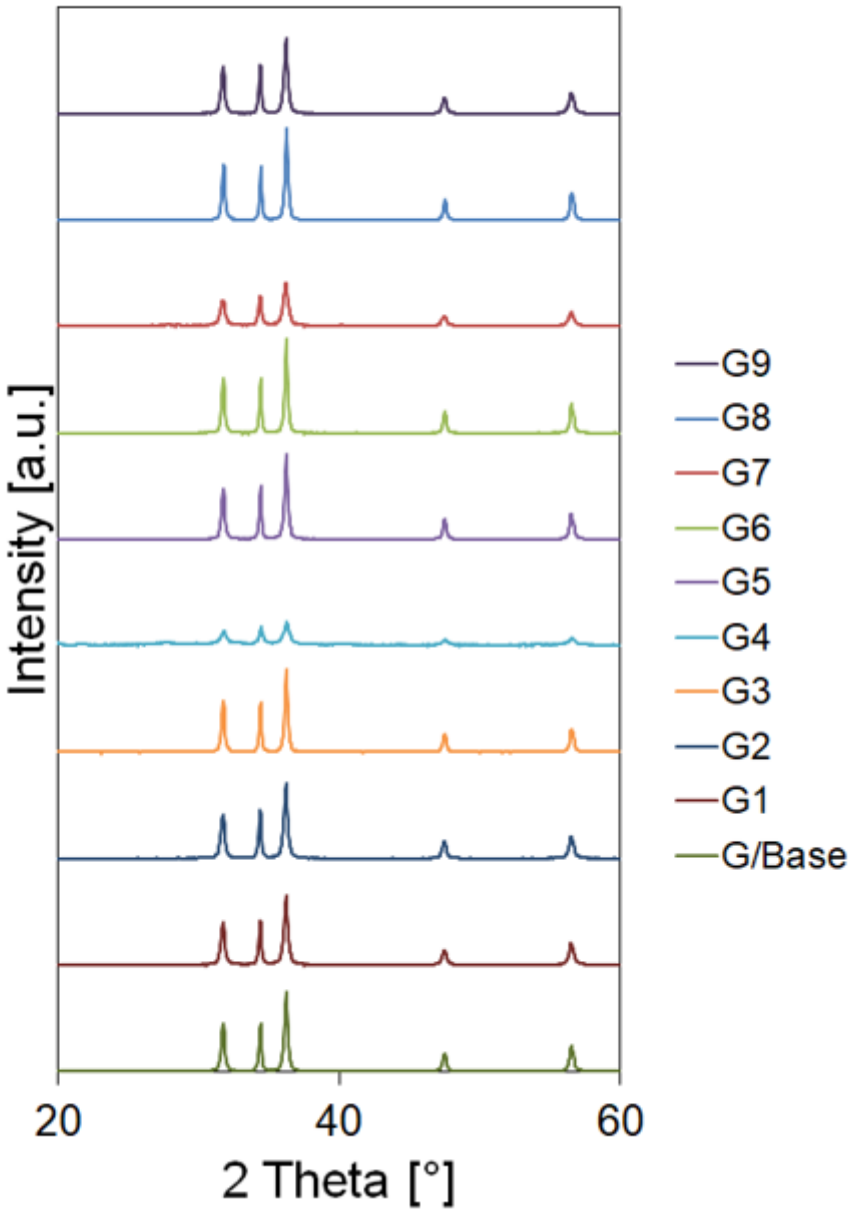

Figure 1

XRD diffractograms indicating obtaining ZnO in all cases

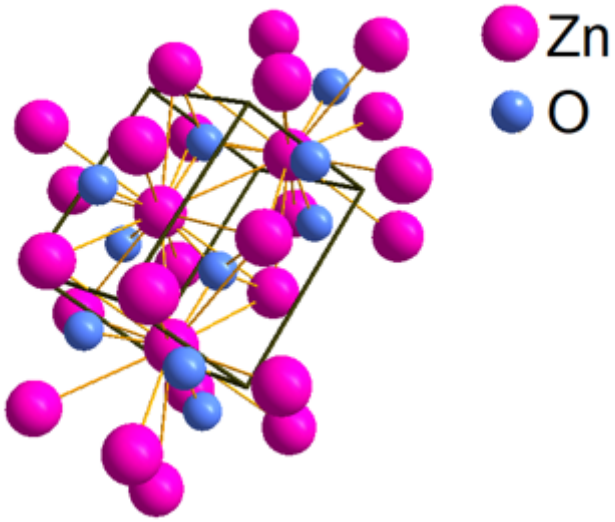

Figure 2

Crystalline elementary cells of ZnO (G3)

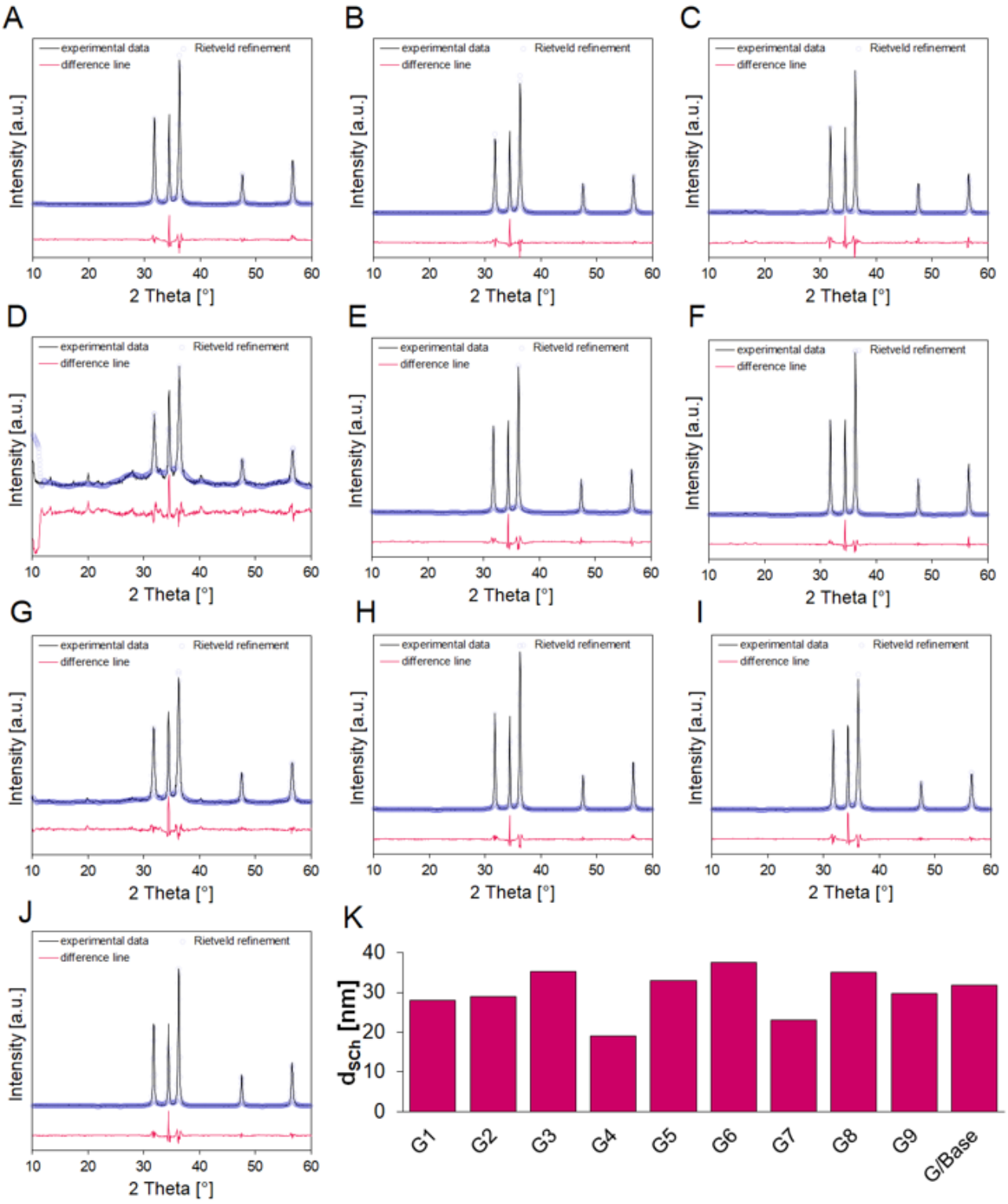

Figure 3

Diffractograms of individual materials with Rietveld matching: A) G1, B) G2, C) G3, D) G4, E) G5, F) G6, G) G7, H) G8, I) G9, J) G/Base, K) crystallites size

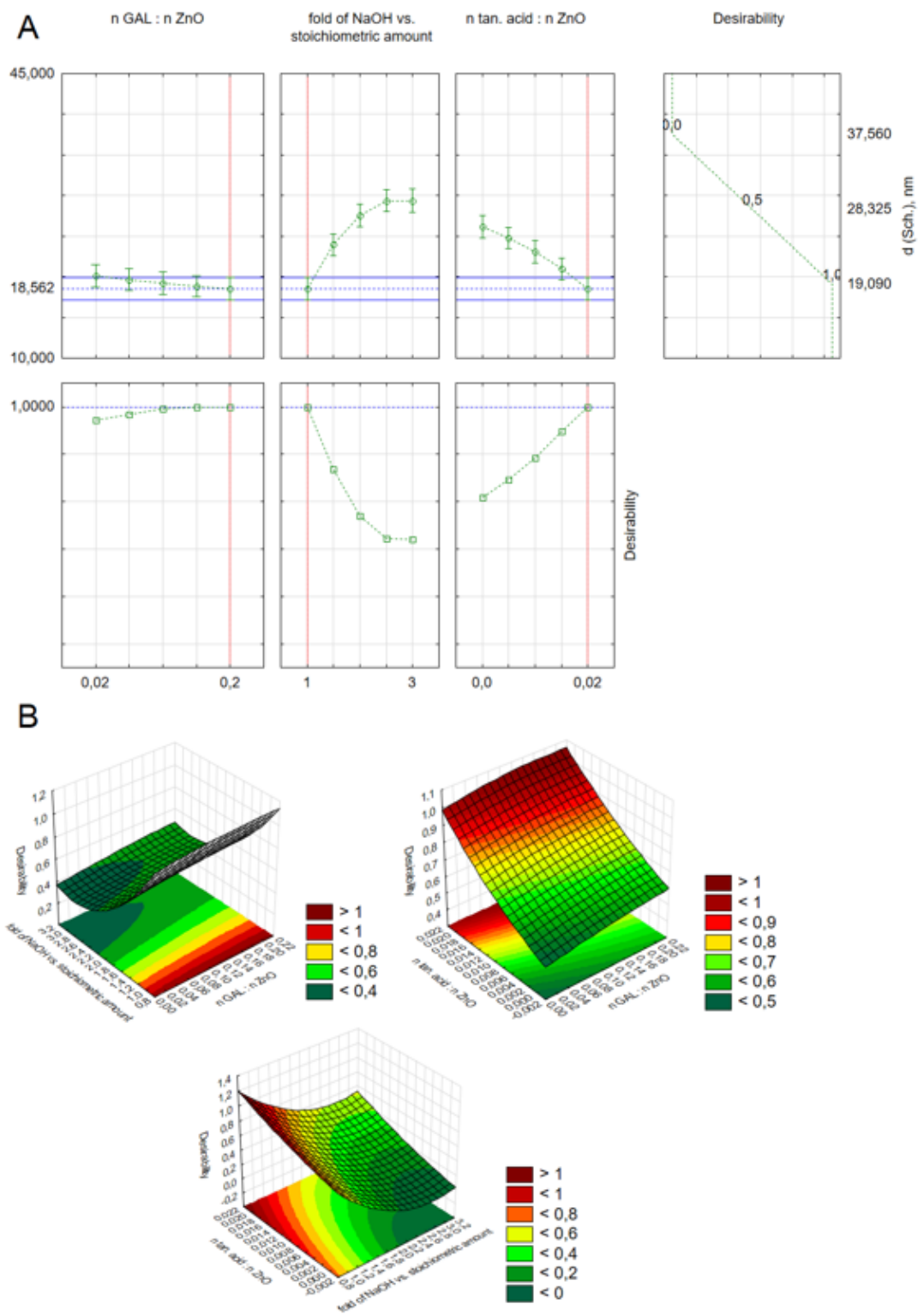

Figure 4

Profiles presenting the dependence of crystallite size on input parameters: A) approximation profiles, B) saddle charts.

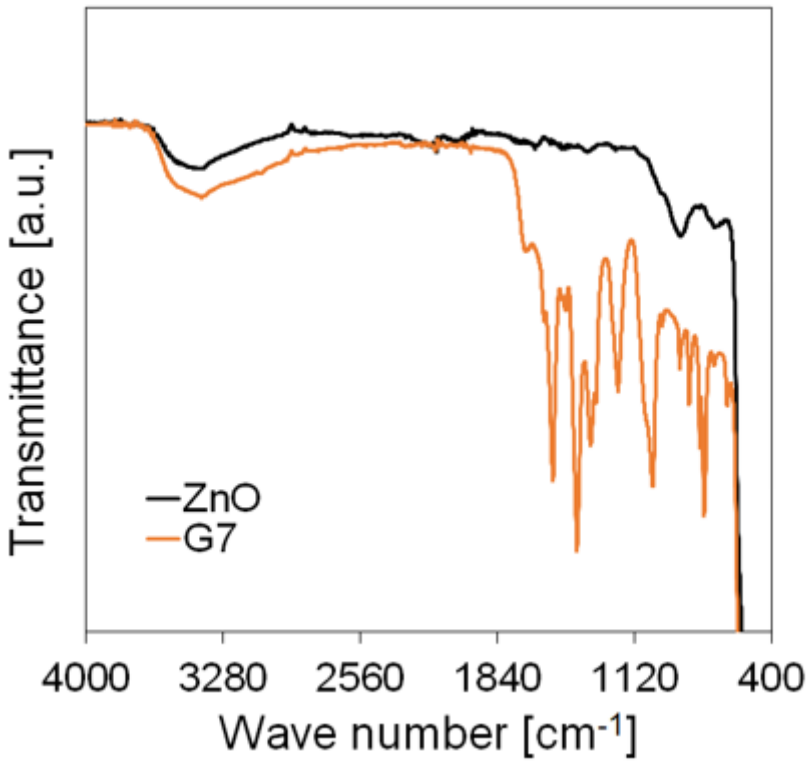

Figure 5

ATR-FTIR spectra of obtained materials

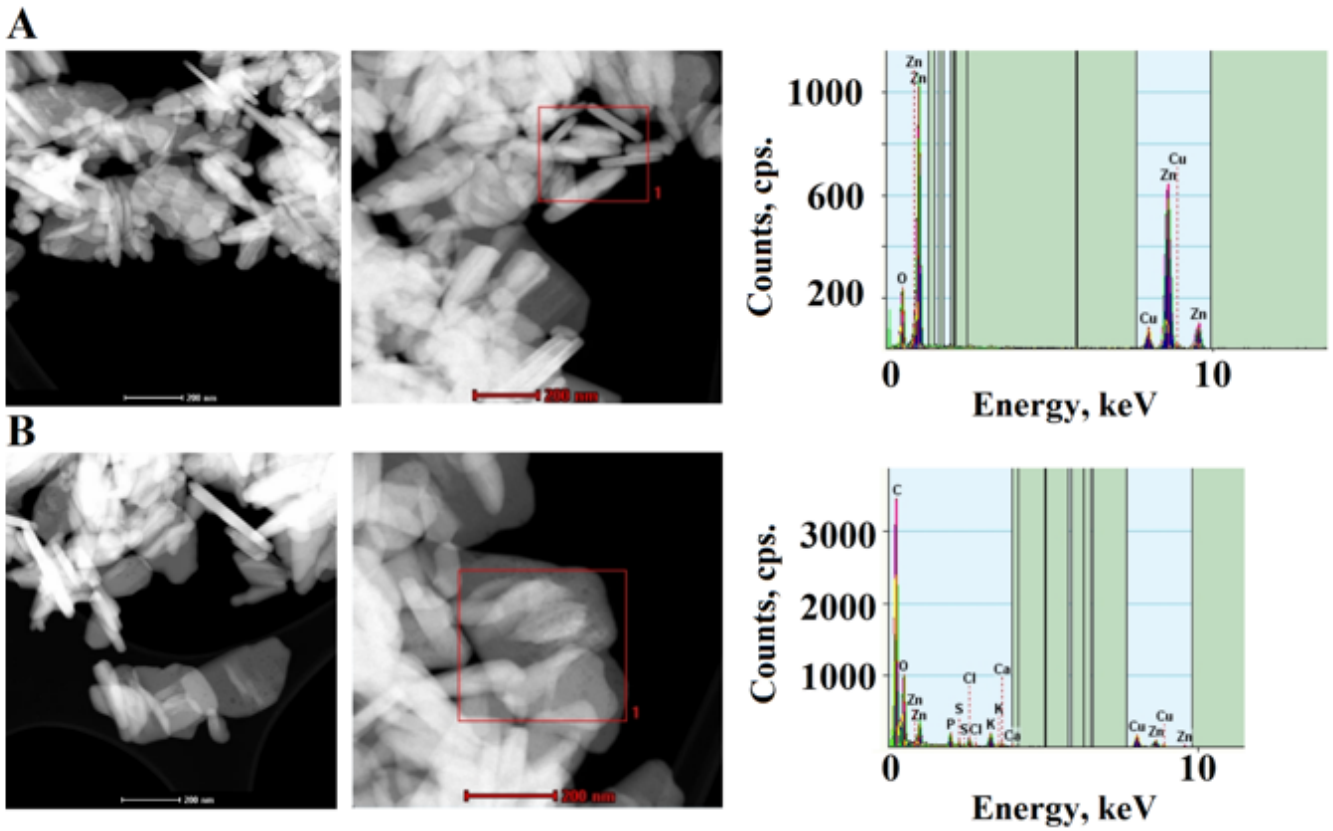

Figure 6

Results of the TEM-EDS analysis: A) G/Base, B) G6

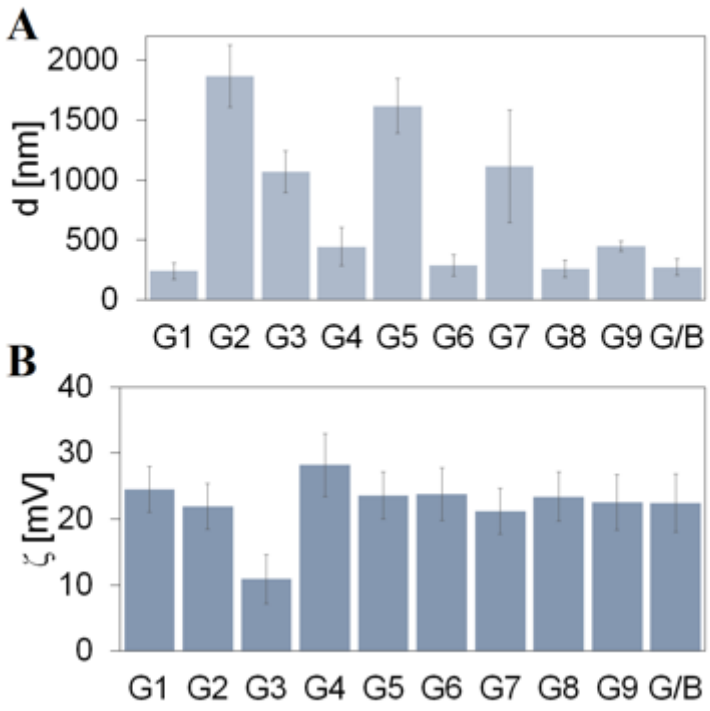

Figure 7

Results of DLS analysis: A) average size, B) electrokinetic potential, zeta

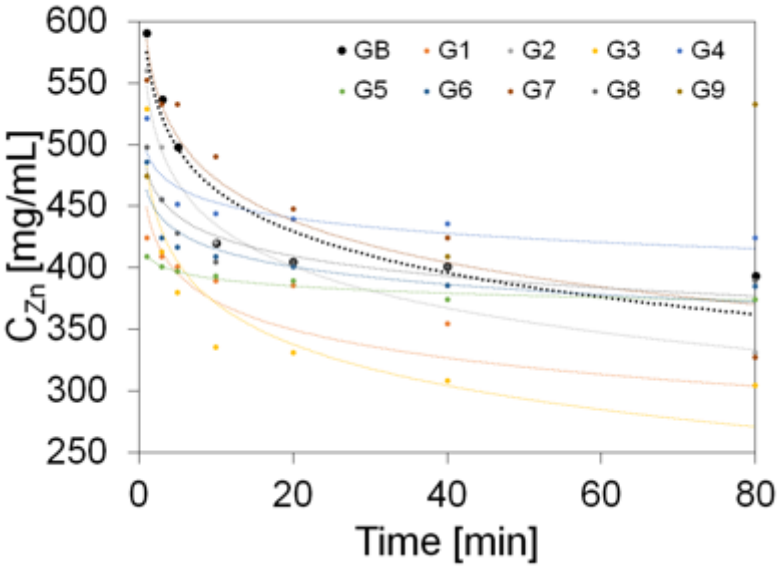

Figure 8

Zinc releasing profiles

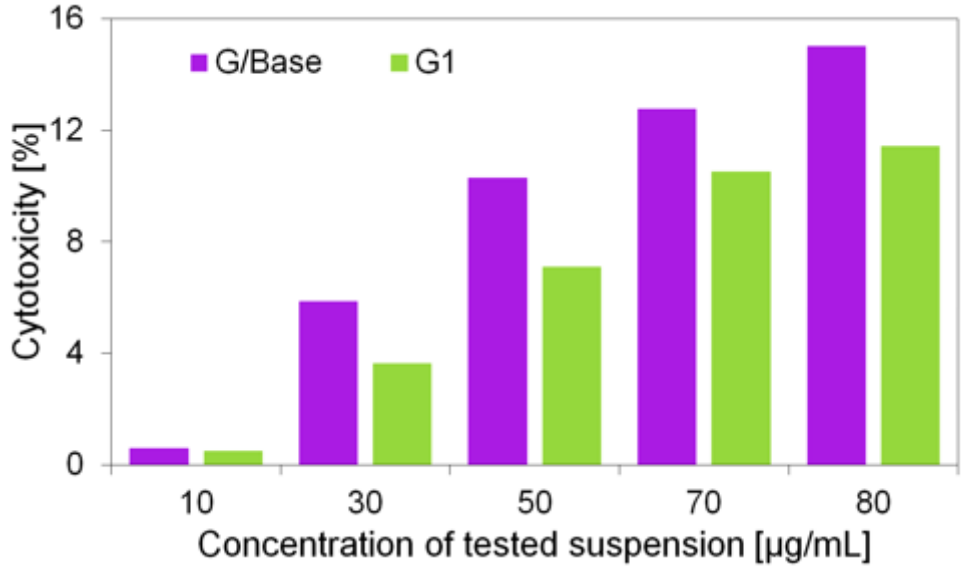

Figure 9

Concentration dependent cytotoxicity of obtained nanoparticles in CHO cells

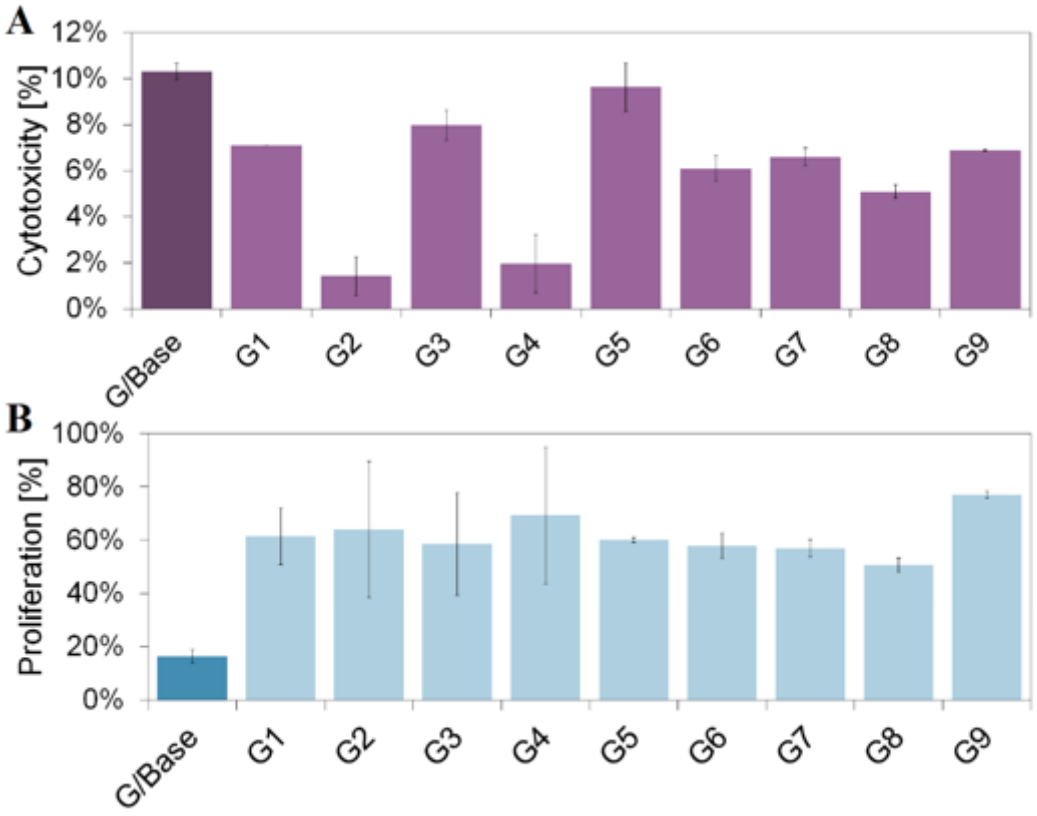

Figure 10

Results of A) cytotoxicity and B) proliferation analysis

Supplementary Files

This is a list of supplementary files associated with this preprint. Click to download.

- Graphicalabstract.png